

# Dynamic Behavior Analysis of a Geometrically Nonlinear Plate Subjected to a Moving Load

A. Mamandi<sup>1,\*</sup>, R. Mohsenzadeh<sup>2</sup>

<sup>1</sup>Department of Mechanical Engineering, Parand Branch, Islamic Azad University, Parand, Iran

<sup>2</sup>Department of Mechanical Engineering, Science and Research Branch, Islamic Azad University, Tehran, Iran

Received 5 March 2019; accepted 4 May 2019

## ABSTRACT

In this paper, the nonlinear dynamical behavior of an isotropic rectangular plate, simply supported on all edges under influence of a moving mass and as well as an equivalent concentrated force is studied. The governing nonlinear coupled PDEs of motion are derived by energy method using Hamilton's principle based on the large deflection theory in conjuncture with the von-Karman strain-displacement relations. Then the Galerkin's method is used to transform the equations of motion into the three coupled nonlinear ordinary differential equations (ODEs) and then are solved in a semi-analytical way to get the dynamical responses of the plate under the traveling load. A parametric study is conducted by changing the size of moving mass/force and its velocity. Finally, the dynamic magnification factor and normalized time histories of the plate central point are calculated for various load velocity ratios and outcome nonlinear results are compared to the results from linear solution. © 2019 IAU, Arak Branch. All rights reserved.

**Keywords** : Moving load; Nonlinear response; Plate; Galerkin's method.

## 1 INTRODUCTION

THE dynamical behavior of elastic bodies like beams or plates under moving loads has been the subject of study of many researchers since late sixties. Due to its increasing applications in the field of structural dynamics, obtaining the vibration characteristics of the beams and plates subjected to moving loads have been very important issue for many years. Some examples of such applications can be addressed as the design of bridges and elevated roadways subjected to moving vehicles, runway of aircrafts and the rocket launcher systems. For such cases certainly the accurate calculation of the dynamic response is necessary for reliable design and hence better performance. Primarily, an extensive study of dynamical characteristics of different structures under moving loads are reported by Fryba [3], but all reported studies are related to the linear behavior of the systems. Later on, the linear and nonlinear dynamics of beams excited by a moving mass have been reported by Kiani et al. [6] and Yanmen [22]. The nonlinear dynamical analysis of an inclined Euler-Bernoulli beam subjected to a moving force has been studied by Mamandi et al. [8]. The nonlinear coupled PDEs of motion have been solved by using the mode

\*Corresponding author.

E-mail address: [am\\_2001h@yahoo.com](mailto:am_2001h@yahoo.com) (A. Mamandi).

summation method. The authors concluded that the quadratic nonlinearity assumption in the mode equations of motion prevails the softening behavior on the dynamic response of the beam. The nonlinear coupled governing PDEs of motion of an inclined Timoshenko beam subjected to moving masses/forces have been solved using Galerkin’s approach via numerical integration methods [8, 9, 10, 11, 12, 13, 14]. A parametric sensitivity analysis referred to the magnitude of the travelling mass or force has been done. The dynamical behavior of plates under the act of moving load or moving mass has been studied by a number of researchers [4, 5, 17, 18, 20, 21, 23]. Linear dynamic responses of plates under the action some types of moving loads have been studied in [2].

In this paper, the effect of the geometric nonlinearity caused by stretching of the mid-plane of a rectangular plate with immovable simply supported on all edges and travelled by a moving mass/force on the dynamic response is investigated. Based on the Hamilton’s principle the governing nonlinear coupled PDEs of motion are derived and then solved applying Glarkin’s method to obtain dynamic response of the plate. In extending the issue of moving mass further to a more applicable study we believe that the same problem but under motion of the moving force has its own importance in this filed. Based on this postulate this study is initiated. It should be mentioned that what makes this work new is related to the very important outcome results from the application point of view. Briefly, it should be pointed out that the main contribution and significant technical advantages of this paper is to present some tangible results which have not been reported in the earlier published papers.

## 2 MATHEMATICAL MODELING

### 2.1 Problem statement

Consider an isotropic and homogenous elastic rectangular plate of sides  $a$  and  $b$  (length  $a$  and width  $b$ ) simply supported on all edges with plate density  $\rho$ , uniform thickness  $h$ , mass per unit area of the plate  $\mu (= \rho h)$ , modulus of elasticity  $E$ , Poisson’s ratio  $\nu$ , bending stiffness  $D = Eh^3/12(1-\nu^2)$  and subjected to a moving mass  $m_e$  with constant velocity  $V$  (in the case of constant velocity of motion) and constant acceleration/deceleration  $A$  (in the case of motion with constant acceleration) as shown in Fig. 1. As can be seen in Fig. 1 the origin of the Cartesian coordinate system  $xoy$  is placed at the lower left corner of the plate. In our upcoming analysis it is assumed that the moving mass travels along a straight line at half of the plate’s width, i.e.  $y = b/2$  (see Fig. 1). It should be mentioned that in our upcoming analysis when the moving mass enters the left side of the plate at time  $t = 0$ , zero initial conditions are assumed. Moreover, in our analysis it has been assumed the moving mass during its travel never loses its contact with the plate surface under it. In this work, the nonlinear dynamic behavior for the coupled longitudinal and transversal in-plane and out of plane displacements of a uniform rectangular plate under the act of moving mass/force is considered. It is assumed that the damping behavior follows the viscous nature. Moreover, the plate deforms within the linear elastic range and therefore the Hook’s law is prevailing.

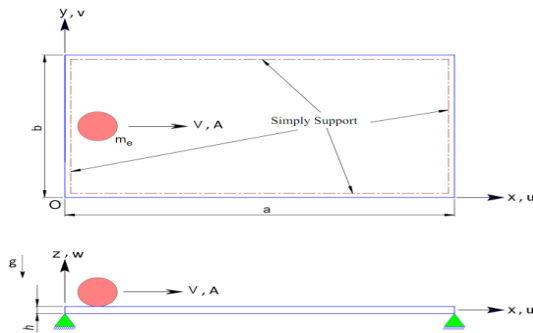


**Fig.1**  
A rectangular plate of sides  $a$  and  $b$  simply supported on all edges subjected to a traveling mass  $m_e$  with velocity  $V$  and acceleration/deceleration  $A$ .

According to the von-Karman nonlinear strain-displacement relations, the normal strains  $\epsilon_x$  and  $\epsilon_y$  and the shearing strain  $\gamma_{xy}$  of the middle surface for the plate shown in Fig. 1 are expressed as follows [16, 19, 23].

$$\epsilon_x = u_{,x} + w_{,x}^2 / 2, \epsilon_y = v_{,y} + w_{,y}^2 / 2, \gamma_{xy} = u_{,y} + v_{,x} + w_{,y} w_{,x} \tag{1}$$

In which  $u(x, y, t)$ ,  $v(x, y, t)$  and  $w(x, y, t)$  represent the time dependent displacements of an arbitrary point

located on the middle surface of plate in  $x$ ,  $y$  and  $z$  directions, respectively measured from equilibrium position when unloaded. Also, in our notation the subscripts  $(,x)$ ,  $(,y)$  and  $(,t)$  stand for the derivative with respect to the spatial coordinates  $(x)$  and  $(y)$  and time  $(t)$ , respectively. To obtain the nonlinear governing differential equations of motion by applying Hamilton's principle, the kinetic energy  $T$  of the rectangular plate under consideration is [15, 16]:

$$T = \frac{1}{2} \rho h \int_0^a \int_0^b (u_{,t}^2 + v_{,t}^2 + w_{,t}^2) dx dy \quad (2)$$

and according to the Kirchhoff's plate hypotheses, the strain energy  $U$  of the plate is given by [15]:

$$U = \frac{1}{2} \int_0^a \int_0^b \int_{-h/2}^{h/2} (\sigma_x \varepsilon_x + \sigma_y \varepsilon_y + \tau_{xy} \gamma_{xy}) dx dy dz \quad (3)$$

where  $\sigma_x$ ,  $\sigma_y$  and  $\tau_{xy}$  are normal and shear in-plane stresses, respectively and for the plate under consideration can be obtained by the Hook's law given by [19]:

$$\sigma_x = \frac{E(\varepsilon_x + \nu \varepsilon_y)}{1 - \nu^2}, \sigma_y = \frac{E(\varepsilon_y + \nu \varepsilon_x)}{1 - \nu^2}, \tau_{xy} = \frac{E \gamma_{xy}}{2(1 + \nu)} \quad (4)$$

Now, we can establish the Lagrangian function of the system as:  $L = T - (U - W_e)$ . Applying Hamilton's principle on  $L$  yield to [15, 23]:

$$\delta \int_{t_1}^{t_2} L dt = 0 \Rightarrow \delta \int_{t_1}^{t_2} (U - T) dt = \int_{t_1}^{t_2} \delta W_e dt \quad (5)$$

In which the total external virtual work done  $\delta W_e$  by the gravity and the travelling mass acting on the plate at the location  $x = x_0(t)$  and  $y = y_0(t) (= b/2)$  is [15, 23]:

$$\delta W_e = - \int_0^b \int_0^a m_e (g + w_{,tt} + 2V w_{,xt} + V^2 w_{,xx} + A w_{,x}) \delta w \Big|_{x_0(t) = \frac{1}{2} A t^2 + V_0 t + x_0, y_0(t) = b/2} dx dy \quad (6)$$

In which,  $m_e w_{,tt}$ ,  $2m_e V w_{,xt}$  and  $m_e V^2 w_{,xx}$  are inertial, Coriolis and centrifugal induced forces acting on the elastic surface of the plate, respectively due to the motion of the mass.

After substitution of Eqs. (2), (3) and (6) into Eq. (5), performing the integration and doing some mathematical simplifications one would get the nonlinear governing coupled PDEs of motion (EOMs) for the force relation in the  $x$ ,  $y$  and  $z$  directions, respectively as follows:

$$u_{,xx} + w_{,x} w_{,xx} + \nu (v_{,xy} + w_{,y} w_{,xy}) + \frac{(1-\nu)}{2} (u_{,yy} + v_{,xy} + w_{,x} w_{,yy} + w_{,y} w_{,xy}) = c_p^{-2} u_{,tt} \quad (7)$$

$$u_{,yy} + w_{,y} w_{,yy} + \nu (u_{,xy} + w_{,x} w_{,xy}) + \frac{(1-\nu)}{2} (u_{,xy} + v_{,xx} + w_{,x} w_{,xy} + w_{,y} w_{,xx}) = c_p^{-2} v_{,tt} \quad (8)$$

$$\frac{1}{12} h^2 \nabla^4 w - u_{,x} w_{,xx} - \frac{1}{2} w_{,x}^2 w_{,xx} - v_{,y} w_{,yy} - \frac{1}{2} w_{,y}^2 w_{,yy} - \nu (v_{,y} w_{,xx} + \frac{1}{2} w_{,y}^2 w_{,xx} + u_{,x} w_{,yy} + \frac{1}{2} w_{,x}^2 w_{,yy}) - (1-\nu) (u_{,y} w_{,xy} + v_{,x} w_{,xy} + w_{,x} w_{,y} w_{,xy}) + \frac{c}{c_p^2 \rho h} w_{,t} = c_p^{-2} (w_{,x} u_{,tt} + w_{,y} v_{,tt} - w_{,tt}) \quad (9)$$

$$- \frac{m_e}{c_p^2 \rho h} \delta(x - x_0(t)) \delta(y - y_0(t)) \times (w_{,xx} V^2 + w_{,tt} + 2w_{,xt} V + w_{,x} A + g) \Big|_{x_0(t) = \frac{1}{2} A t^2 + V_0 t + x_0, y_0(t) = b/2}$$

In which  $c_p^2 = E/\rho(1-\nu^2)$  and  $\nabla^4 = (\partial^4/\partial x^4 + 2\partial^4/\partial x^2\partial y^2 + \partial^4/\partial y^4)$ . Furthermore,  $\delta(x-x_0(t))\delta(y-y_0(t))$  represents two dimensional Dirac's delta function in which  $x_0(t)$  and  $y_0(t)$  are the instantaneous position of the moving mass travelling on the plate. In case the mass is travelling with a constant velocity  $V$  ( $A = 0$ ) on a straight path along the trajectory parallel to the side  $a$  at the half of the width of the plate ( $y = b/2$ ), then its instantaneous position is given by  $x_0(t) = Vt + x_0$  and  $y_0(t) = b/2$  where  $x_0$  represents the initial position of the mass at the start of its motion. In addition,  $c$  (or  $c_{m,n}$ ) coefficient is internal viscous damping of the plate related to modal damping ratio, namely  $\zeta_{m,n}$  expressed by  $\zeta_{m,n} = c_{m,n}/2(\lambda_{m,n}\omega_{m,n})$  [1, 23], where  $\omega_{m,n}$  is the natural frequency of the  $m$ th- $n$ th mode of vibration and  $\lambda_{m,n}$  is the modal mass of this mode given by  $\lambda_{m,n} = \rho h a b / 4$  [1,7].

### 3 SOLUTION METHOD

In this study Galerkin's method is chosen as a powerful mathematical tool to analyze the vibrations of a plate. Based on the separation of variables technique, the response of the plate in terms of the linear free-oscillation modes can be assumed as follows: [1]

$$u(x, y, t) = \sum_i^m \sum_j^n p_{ij}(t) \phi_{ij}(x, y) = P(t) \Phi^T(x, y) \tag{10}$$

$$v(x, y, t) = \sum_k^m \sum_l^n q_{kl}(t) \psi_{kl}(x, y) = Q(t) \Psi^T(x, y) \tag{11}$$

$$w(x, y, t) = \sum_v^n \sum_z^M r_{vz}(t) \theta_{vz}(x, y) = R(t) \Theta^T(x, y), \tag{12}$$

where  $P(t)$ ,  $Q(t)$  and  $R(t)$  are vectors listing the generalized coordinate  $p_{ij}(t)$ ,  $q_{kl}(t)$  and  $r_{vz}(t)$ , respectively and  $\Phi(x, y)$ ,  $\Psi(x, y)$  and  $\Theta(x, y)$  are some vectorial functions collecting the first mode shapes (eigen-functions) of  $\phi_{ij}(x, y)$ ,  $\psi_{kl}(x, y)$  and  $\theta_{vz}(x, y)$ , respectively. In the next step, primarily we substitute Eqs. (10) to (12) into Eqs. (7), (8) and (9), then on the resulting relations, pre-multiplying both sides of Eq. (7) by  $\Phi^T(x, y)$ , Eq. (8) by  $\Psi^T(x, y)$  and Eq. (9) by  $\Theta^T(x, y)$ , integrating over the interval  $(0, a)$  and  $(0, b)$  and imposing the orthogonality property of the vibration modes of the plate along with the properties of the two dimensional Dirac delta function, the resulting nonlinear coupled modal ODEs of motion in matrix form are as follows:

$$i = l = 2, 4, \dots, m, j = k = 1, 2, \dots, n, v = 1, 2, \dots, M \text{ and } z = 1, 2, \dots, N$$

$$c_p^{-2} \sum_{i,j}^{m,n} I_{7,ij} \ddot{p}_{ij}(t) - \sum_{i,j}^{m,n} (I_{1,ij} + \frac{1}{2}(1-\nu)I_{5,ij}) p_{ij}(t) - \frac{1}{2}(1+\nu) \sum_{k,l}^{n,m} \sum_{i,j}^{m,n} I_{3,kl ij} q_{kl}(t) - \sum_{v,z}^{M,N} \sum_{i,j}^{m,n} (I_{2,vz ij} + \frac{1}{2}(1+\nu)I_{4,vz ij} + \frac{1}{2}(1-\nu)I_{6,vz ij}) r_{vz}^2(t) = 0 \tag{13}$$

$$c_p^{-2} \sum_{k,l}^{n,m} I_{14,kl} \ddot{q}_{kl}(t) - \sum_{k,l}^{n,m} (I_{8,kl} + \frac{1}{2}(1-\nu)I_{12,kl}) q_{kl}(t) - \frac{(1+\nu)}{2} \sum_{i,j}^{m,n} \sum_{k,l}^{n,m} I_{10,ijkl} p_{ij}(t) - \sum_{v,z}^{M,N} \sum_{k,l}^{n,m} I_{9,vz kl} + \frac{(1+\nu)}{2} I_{11,vz kl} + \frac{(1-\nu)}{2} I_{13,vz kl} r_{vz}^2(t) = 0 \tag{14}$$

$$\sum_{v,z}^{M,N} (\frac{m_e}{c_p^2 \rho h} I_{34,vz} + c_p^{-2} I_{31,vz}) \ddot{r}_{vz}(t) + \sum_{v,z}^{M,N} (2m_e V I_{35,vz} + \frac{c_{m,n}}{c_p^2 \rho h} I_{31,vz}) \dot{r}_{vz}(t) + \sum_{v,z}^{M,N} [\frac{h^2}{12} (I_{15,vz} + 2I_{16,vz} + I_{17,vz}) + \frac{m_e V^2}{c_p^2 \rho h} I_{33,vz} + \frac{m_e A}{c_p^2 \rho h} I_{35,vz}] r_{vz}(t) - \sum_{v,z}^{M,N} [\frac{1}{2} (I_{19,vz} + I_{21,vz} + \nu(I_{23,vz} + I_{25,vz})) + (1-\nu)I_{28,vz}] r_{vz}^3(t) + \sum_{i,j}^{m,n} \sum_{v,z}^{M,N} [(I_{18,ijvz} + \nu I_{24,ijvz} + (1-\nu)I_{26,ijvz}) p_{ij}(t) + c_p^{-2} I_{29,ijvz} \ddot{p}_{ij}(t)] r_{vz}(t) + \sum_{k,l}^{n,m} \sum_{v,z}^{M,N} [(I_{20,klvz} + \nu I_{22,klvz} + (1-\nu)I_{27,klvz}) q_{kl}(t) + c_p^{-2} I_{30,klvz} \ddot{q}_{kl}(t)] r_{vz}(t) = \frac{m_e g}{c_p^2 \rho h} \sum_{v,z}^{M,N} I_{32,vz} \tag{15}$$

In which dot mark over any parameter indicate the derivative with respect to the time, ( $t$ ). All matrices  $I_1$  to  $I_{35}$  appearing in above relations are given in Appendix A. It is clear that Eqs. (13) to (15) are three nonlinear coupled second-order ordinary differential equations (ODEs). The boundary conditions for a plate with immovable simply supported on all edges and initial conditions (ICs) are: [19]

$$\begin{aligned} \text{Essential BCs: } u = v = w = 0 & \quad \text{at } x = 0, a & \quad u = v = w = 0 & \quad \text{at } y = 0, b \\ \text{Natural BCs: } M_x = 0 \rightarrow w_{,xx} = 0 & \quad \text{at } x = 0, a & \quad M_y = 0 \rightarrow w_{,yy} = 0 & \quad \text{at } y = 0, b \end{aligned} \quad (16)$$

and

$$\text{ICs } u(x, y, 0) = u_{,t}(x, y, 0) = v(x, y, 0) = v_{,t}(x, y, 0) = w(x, y, 0) = w_{,t}(x, y, 0) = 0 \quad (17)$$

The equations of motions for a plate subjected to a moving concentrated force of magnitude  $m_e g$  can be derived from the equations of motion for a plate subjected to a moving mass by neglecting the inertial effect of the traveling mass. For this system the Eqs. (9) and (15) are needed to be rewritten where Eqs. (7), (8), (13) and (14) remain unchanged.

In order to solve the Eqs. (13), (14) and (15), all entries in the matrices listed in Appendix A should be calculated. It can be seen that the following functions (mode shapes) for the  $\phi_{ij}(x, y)$ ,  $\psi_{kl}(x, y)$  and  $\theta_{z}(x, y)$  will satisfy both the linearized equations of motion and boundary conditions of the plate with immovable simply supported on all edges [1].

$$\phi_{ij}(x, y) = \sin \frac{i \pi x}{a} \sin \frac{j \pi y}{b}, \psi_{kl}(x, y) = \sin \frac{k \pi x}{a} \sin \frac{l \pi y}{b}, \theta_z(x, y) = \sin \frac{v \pi x}{a} \sin \frac{z \pi y}{b} \quad (18)$$

Now, we use Eq. (18) to calculate all matrix quantities given in Appendix A. In the next step these evaluated matrices will be used in the Eqs. (13) to (15) and later the set of equations will be solved numerically using the Adams-Bashforth-Moulton integration method via MATLAB solver package to obtain values of  $p_{ij}(t)$ ,  $q_{kl}(t)$  and  $r_{z}(t)$ . By back substitution of  $p_{ij}(t)$ ,  $q_{kl}(t)$  and  $r_{z}(t)$  in Eqs. (10) to (12),  $u(x, y, t)$ ,  $v(x, y, t)$  and  $w(x, y, t)$  can be obtained, respectively. Subsequently, after obtaining values for  $u(x, y, t)$ ,  $v(x, y, t)$  and  $w(x, y, t)$  the dynamic response of the rectangular plate subjected to a moving mass travelling with a constant velocity can be calculated. Moreover, the dynamic response of the rectangular plate under variation of different parameters, including the velocity of the moving mass or an equivalent force and magnitude of the moving load are discussed.

#### 4 RESULTS AND DISCUSSIONS

To establish our calculations we consider a plate with geometry and mechanical properties listed in below:

$$a = 4m, b = 2m, h = 0.01m, E = 200 \times 10^9 Pa, \rho = 7850 kg / m^3, g = 9.81m / s^2, \zeta = 0.033 \text{ and } \nu = 0.3 \quad (18)$$

It should be mentioned that all deflection variation vs. moving mass instantaneous position are given in a non-dimensional form that is  $w/w_{static}$ . Moreover, it has to be pointed out that based on the conducted convergence study related to the linear and nonlinear analyses, 9 modes of vibration are taken into account for the steady state answers for  $u(x, y, t)$ ,  $v(x, y, t)$  and  $w(x, y, t)$ . To clarify the results and in order to have a better insight on interpreting the variation of the obtained results we tried to present the results in dimensionless forms. So we begin with defining the dynamic magnification factor D.M.F. as the ratio of absolute maximum dynamic vertical deflection of the central point of the plate to its maximum static response at the same point. The static deflection of the plate's center point under a concentrated mass applied at the same point is equal to  $w_{static} = 0.01651 m_e g a^2 / D$  [19]. Moreover let's define the velocity ratio as  $\alpha = T_1 / T = V / V_p$  in which  $V_p = a / T_1 = \omega_n a / 2\pi$ , where  $T_1$ ,  $T$  and  $V_p$  denote the first natural period (fundamental period of transverse motion) of the plate, the total time taken by the moving load to cross from one side to the opposite side of plate and the velocity of a reference load that would take the time of  $T_1$  to traverse the plate of length  $a$ , respectively. Moreover,  $\omega_n$  is the natural frequency of plate given by:

$$\omega_n = \omega_{ij} = \pi^2 \left[ \left( i / a \right)^2 + \left( j / b \right)^2 \right] \sqrt{D / \rho a b}, \text{ in which } i, j = 1, 2, \dots, n.$$

Based on the given data, the analysis for D.M.F. was conducted for both linear and nonlinear solutions and its variation vs.  $\alpha$  for different values of the moving mass ratios while the mass has not left the beam is depicted in Fig. 2. From this figure it can be seen that by increasing the magnitude of the moving mass, the dynamic deflection response of the plate grows in such way that does not follow the well-known linear trend. Moreover, the significant difference between the linear and nonlinear solutions is always seen. For example it can be observed that for  $m_e = 0.5\mu ab$ , the value of D.M.F. of the linear and nonlinear solutions yields 1.75 and 2.1 at  $\alpha = 1.55$  and  $\alpha = 1.15$ , respectively. Meanwhile, in the region  $0 < \alpha < 0.5$  another maximum is seen around  $\alpha = 0.4$  and similar differences between linear and nonlinear analyses as described above exists in this region. Briefly, in the under critical region ( $\alpha \leq 1.2$ ) the nonlinear dynamic deflection of the plate generally increases by increasing the velocity of moving mass and in the overcritical region ( $\alpha > 1.2$ ) the nonlinear dynamic deflection decreases by increasing the velocity of moving mass. In addition, as a significant phenomenon, it can be observed that by increasing the magnitude of the moving mass ratios, the maximum D.M.F. for the linear and nonlinear solutions occurs in the lower values of  $\alpha$  no matter what type of analysis is used.

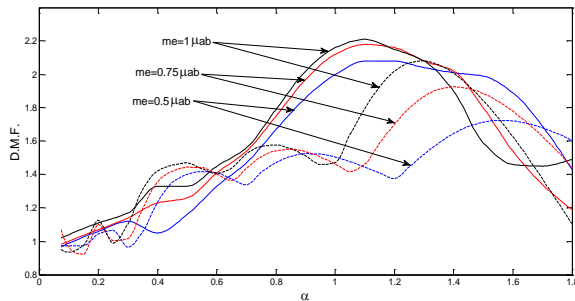


**Fig.2**  
Variation of dynamic magnification factor (D.M.F.) vs.  $\alpha$  for a rectangular plate affected by a moving mass of  $m_e$  (kg); (—) nonlinear analysis, (----) linear analysis.

By employing Eqs. (7), (8), (9), (13), (14) and (15) one can obtain the variation of the dynamic magnification factor DMF vs.  $\alpha$  by changing the equivalent concentrated moving force  $F$ . Fig. 3 represents such variations of the D.M.F. for the central point of a plate under the act of several equivalent moving forces using nonlinear and as well as the linear analysis. It can be seen that by increasing the magnitude of the vertical moving Force  $F$ , the dynamic displacement response of the plate grows in such way that does not follow the well-known linear force-deflection relation in the linear systems, i.e.,  $F = k\delta$ . Also it can be observed that the dynamic displacement response of the linear and nonlinear solutions is almost the same for  $F \leq 0.05\mu gab$  N no matter what the value of  $\alpha$  would be. For the same value of  $F$  the maximum D.M.F. for linear and nonlinear solutions are the same and equal to 1.48 and 1.47 at  $\alpha = 1.3$ , respectively. Moreover, as the value of  $F$  increase, i.e., for  $F > 0.05\mu gab$  N, the difference between the linear and nonlinear dynamic response become more distinct whereas for  $F = \mu gab$  N at  $\alpha \approx 1.5$ , this difference has its maximum value of 0.31 which have about 21% difference. In addition, it can be seen from this figure that for all value of  $F$  and  $\alpha$ , the linear solution predicts almost a lower value for D.M.F. Contrary to what is seen in Fig. 2 it should be noted that in Fig. 3 the linear equivalent moving force analysis always predicts a unique value for D.M.F. no matter the value of  $F$  would be. Moreover, by increasing the magnitude of the moving force ratios, the maximum value of D.M.F. for the nonlinear solution occurs in the higher value of  $\alpha$ . Briefly, in the under critical region ( $\alpha \leq 1.8$ ) the dynamic central point deflection of the plate generally increases by increasing the velocity of moving force and in the overcritical region ( $\alpha > 1.8$ ) the dynamic deflection decreases by increasing the velocity of moving force. It should be pointed out that similar behavior as can depicted in Figs. 2 and 3 can be seen in a beam traveled by moving loads as reported in literature [8, 10, 11, 12].

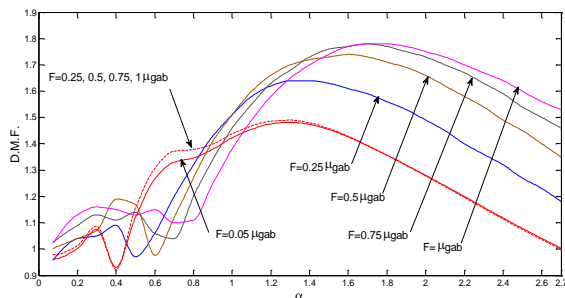


**Fig.3**  
Variation of dynamic magnification factor (D.M.F.) vs.  $\alpha$  for rectangular plate under motion of a concentrated moving force of  $F$  (N); (—) nonlinear analysis, (----) linear analysis.

Figs. 4(a-b) show the effect of damping ratio on the dynamic behavior of central point of plate under moving mass of  $m_e = 0.25\mu ab$  (kg) and an equivalent concentrated force of  $F = 0.25\mu gab$  (N) using nonlinear analysis, respectively. Three different values of  $\zeta = 0$  (undamped condition), 0.033 and 0.066 have been considered [8]. From this figure it can be observed that by increasing the value of damping ratio  $\zeta$  the dynamic displacement decrease which is generally a natural phenomenon in any structural system [8]. Moreover, for the considered parameters, the maximum value of D.M.F. for the moving mass problem decreases from 1.86 (related to  $\zeta = 0$ ) to 1.77 (related to  $\zeta = 0.066$ ) at  $\alpha = 1.2$  (see Fig. 4(a)), whereas for the moving force problem decreases from 1.64 (related to  $\zeta = 0$ ) to 1.56 (related to  $\zeta = 0.066$ ) at  $\alpha = 1.3$  (see Fig. 4(b)).

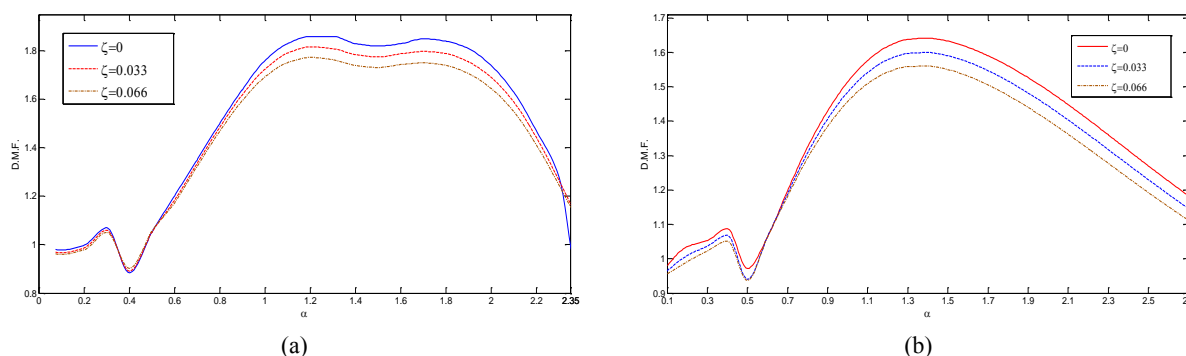


**Fig.4**

Variation of dynamic magnification factor (D.M.F.) vs.  $\alpha$  for central point of a rectangular plate under (a) a moving mass  $m_e = 0.25\mu ab$  (kg) and (b) an equivalent concentrated force of  $F = 0.25\mu gab$  (N) for various damping ratio using nonlinear analysis; (—)  $\zeta = 0$ , (-----)  $\zeta = 0.033$ , (-.-.-.-)  $\zeta = 0.066$ .

In Fig. 5, the maximum dynamic response ( $w$ ) variation of the central point of plate vs. different values of mass ratio  $\eta$  ( $\eta = m_e/\mu ab$ ) is shown for various velocity ratios of  $\alpha = 0.25, 0.5, 0.75, 1, 1.25$  and  $1.5$ , respectively, using both linear and nonlinear solutions. It can be seen that the maximum dynamic deflection of the nonlinear analysis is always lower than the one obtained from the linear solution. This regressive incident which is known as the hardening behavior is mostly due to the existence of the coupled cubic-quadratic nonlinearity characteristic in the equations of motion of the plate where in the other literature it is known as the equivalent to a nonlinear hard spring [8]. In addition, it can be seen from Figs. 5(a-b) that the maximum dynamic displacement of central point of the plate using linear and nonlinear solutions are almost the same for value of  $\eta < 0.1$  in lower velocity ratios. However, after this point the difference between linear and nonlinear analyses for dynamic displacement of central point grow slowly up to  $\eta = 0.4$  (see Figs. 5(c-d)). However, after this point, the magnitude of  $w$  of the nonlinear and linear solutions grows rapidly as the value of  $\eta$  increase (see Figs. 5(e-f)). Moreover, from this figure it can be observed that the difference between the linear and nonlinear solutions has an increasing trend up to the load velocity ratio of  $\alpha = 1.25$  and a reverse trend afterward. It should be noted that the maximum difference between linear and nonlinear solutions for all cases in this figure occurs at  $\eta = 1.5$  at  $\alpha = 1.25$  (see Fig. 5(e)).

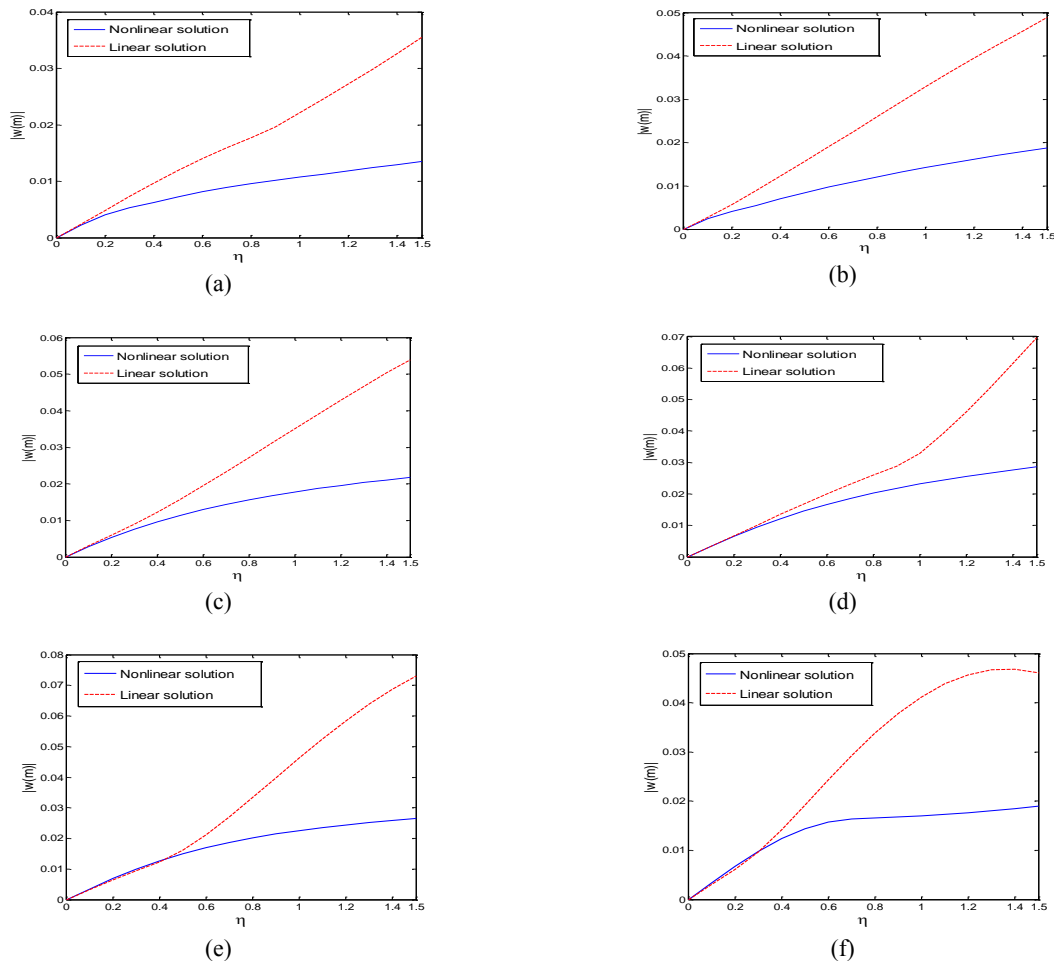
The maximum dynamic displacement variation ( $w$ ) of central point of plate vs. different value of the force ratios  $\eta$  ( $\eta = F/\mu gab$ ) for different velocity ratio of  $\alpha = 0.25, 0.5, 0.75, 1, 1.25$  and  $1.5$ , respectively using both linear and nonlinear approaches are depicted in Figs. 6(a-f). It can be seen that the maximum deflection of the nonlinear analysis is always lower than the one obtained from the linear solution. As it was stated for Fig. 5, this incident is known as the hardening behavior. Also, it is seen from this figure that the maximum dynamic central point displacements of the plate using linear and nonlinear solutions are almost the same for the value of  $\eta < 0.1$ . However, after this point, the magnitude of  $w$  of the nonlinear and linear solutions differs obviously and the difference grows rapidly as the value of  $\eta$  increases. Also, it can be observed from Fig. 6 that the difference between the linear and nonlinear solutions has an increasing trend up to the load velocity ratio of  $\alpha = 1$  and a reverse trend afterward. It should be noted that the maximum difference between linear and nonlinear solutions for all cases in this figure occurs at  $\eta = 1$  at  $\alpha = 1$  (see Fig. 6(d)). Moreover by comparison of Figs. 5 and 6 it can be seen that variation of the linear solution almost mathematically follows a linear trend in Fig. 6, whereas this variation does not represent a linear trend in Fig. 5.

Fig. 7 shows the variation of normalized vertical dynamic displacement ( $W = w_d/w_{static}$ ) of a rectangular plate under the moving mass of  $m_e = 0.25\mu ab$  and as well as an equivalent concentrated moving force of  $F = 0.25\mu gab$  vs. normalized instantaneous mass position, i.e.,  $x = Vt/a$ , for different velocity ratios of  $\alpha = 0.25, 1$  and  $1.25$ ,

respectively using nonlinear analysis. From this figure, it can be seen that there are significant discrepancies between the deflection under the moving mass and the deflection under the equivalent concentrated moving force, especially toward the later part of the motion. Moreover, it can be observed from Fig. 7 that the maximum vertical dynamic displacement of the plate has an increasing trend up to velocity ratio  $\alpha = 1.25$ . Also, it can be seen from this figure that the position of the maximum normalized vertical dynamic displacement of plate at velocity ratio  $\alpha = 0.25$  occurs at the time when the moving mass or an equivalent concentrated moving force is in the middle of the plate length, whereas after this velocity ratio ( $\alpha > 0.25$ ), this position happens at the time of passing the middle point of the plate.

In Fig. 8, the variation of the D.M.F. vs.  $\alpha$  for different values of the rectangular plate's aspect ratio  $AR=3, 4$  and  $5$  ( $AR = a/b$ ) subjected to a traveling mass size of  $m_e = 0.25\mu ab$  (kg) using nonlinear analysis is depicted. From this figure it can be observed that by increasing the aspect ratio of the rectangular plate, the maximum value of the dynamic magnification factor decreases and occurs in the lower values of  $\alpha$ . Now, we investigate the case that any variation on the plate's aspect ratio does not change the total mass of the plate. So, dimensions of a plate with  $AR = 3, 4$  and  $5$  is determined in such a manner that the total mass of the plate remains unchanged with respect to the mass of plate of  $AR = a/b = 2$  as the reference.

Fig. 9 shows the variation of the D.M.F. vs.  $\alpha$  for different values of the plate's aspect ratios  $AR = 3, 4$  and  $5$  subjected to the traveling mass size of  $m_e = 0.25\mu ab$  (kg) using nonlinear analysis where the total mass of the plate remains unchanged. From this figure it can be observed that by increasing the aspect ratio of the rectangular plate, the maximum value of the dynamic magnification factor decreases and contrary to what is seen in Fig. 8 the maximum value of the dynamic magnification factor occurs in the higher values of  $\alpha$ .



**Fig.5** Variation of the dynamic response of the central point of plate  $w$  (m) vs. different values of the mass ratios  $\eta$  for different velocity ratios; (a)  $\alpha = 0.25$ , (b)  $\alpha = 0.5$ , (c)  $\alpha = 0.75$ , (d)  $\alpha = 1$ , (e)  $\alpha = 1.25$ , (f)  $\alpha = 1.5$ ; (—) nonlinear analysis, (-----) linear analysis.

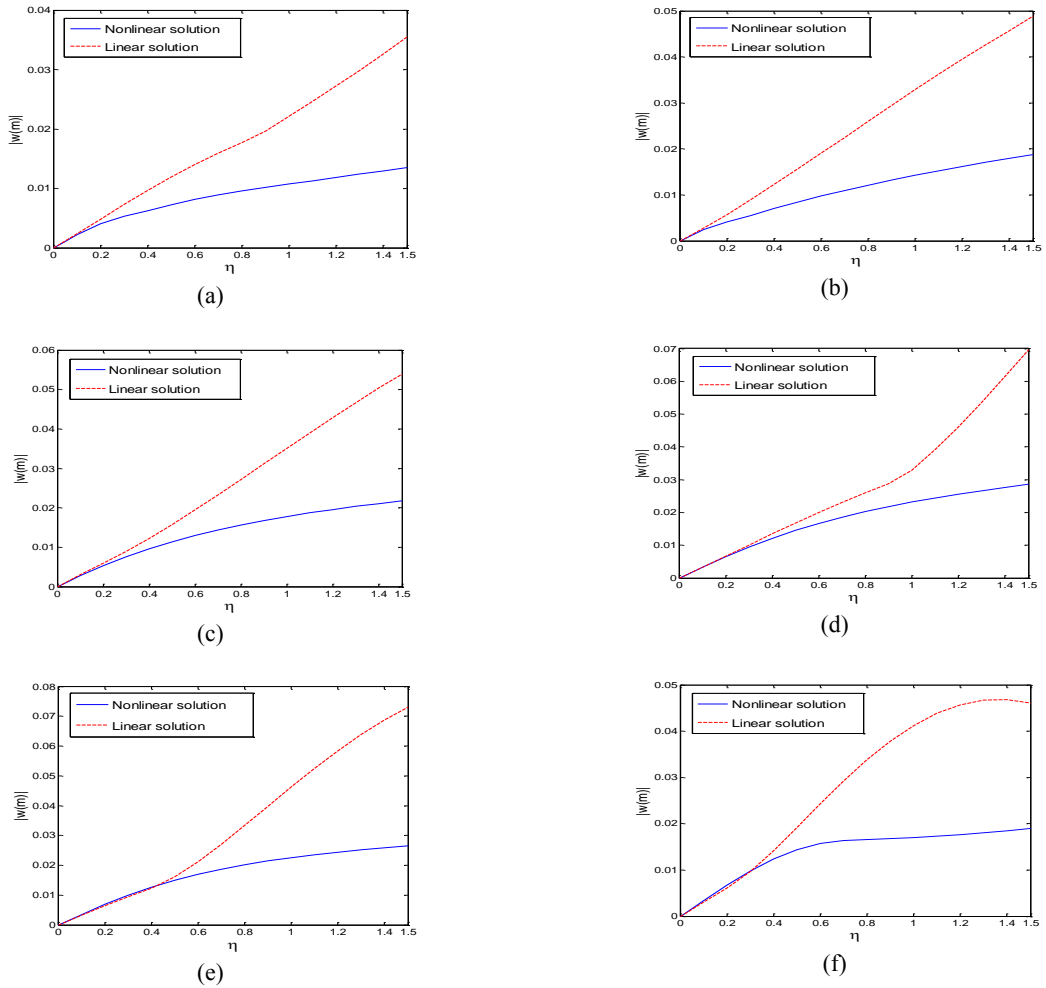


**Fig.6** Variation of the dynamic response of the central point of plate  $w (m)$  vs. different values of the force ratios  $\eta$  for different velocity ratios; (a)  $\alpha = 0.25$ , (b)  $\alpha = 0.5$ , (c)  $\alpha = 0.75$ , (d)  $\alpha = 1$ , (e)  $\alpha = 1.25$ , (f)  $\alpha = 1.5$ ; (—) nonlinear analysis, (----) linear analysis.

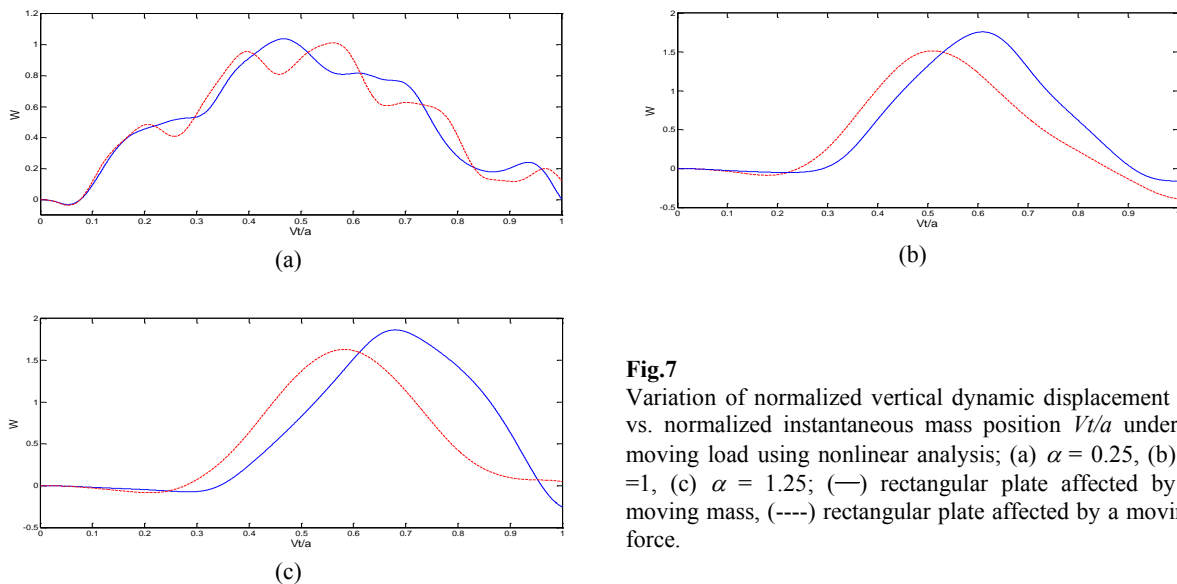


**Fig.7** Variation of normalized vertical dynamic displacement  $W$  vs. normalized instantaneous mass position  $Vt/a$  under a moving load using nonlinear analysis; (a)  $\alpha = 0.25$ , (b)  $\alpha = 1$ , (c)  $\alpha = 1.25$ ; (—) rectangular plate affected by a moving mass, (----) rectangular plate affected by a moving force.

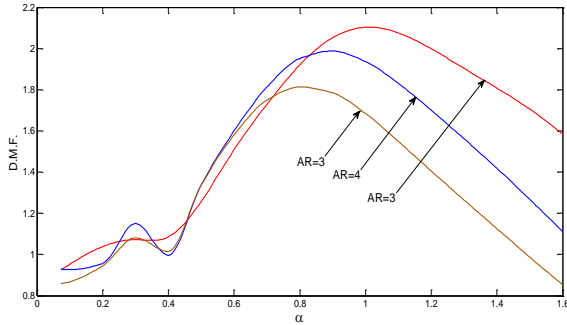


**Fig.8**  
Variation of dynamic magnification factor (D.M.F.) for central point of a rectangular plate vs.  $\alpha$  affected by a moving mass of  $m_e = 0.25\mu ab$  (kg) for various plate's aspect ratios using nonlinear analysis.

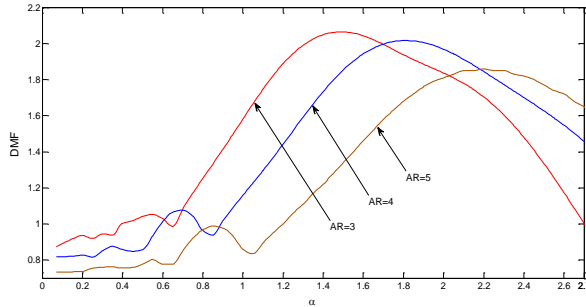


**Fig.9**  
Variation of dynamic magnification factor (D.M.F.) for central point of a rectangular plate vs.  $\alpha$  affected by a moving mass of  $m_e = 0.25\mu ab$  (kg) for various plate's aspect ratios when the total mass of the plate remains unchanged using nonlinear analysis.

Figs. 10(a) and (b) represent the variation of  $w/a$  of the central point of plate under the moving mass value of  $m_e = 0.25\mu ab$  and as well as an equivalent concentrated moving force value of  $F = 0.25\mu gab$  vs.  $Vt/a$  for different velocity ratios  $\alpha = 0.25, 0.5, 0.75, 1, 1.25, 1.5, 1.75, 2$  and  $2.5$  using linear and nonlinear analysis, respectively. From this figure, one can conclude that the results for the vertical dynamic displacement obtained by the nonlinear analysis almost represent smaller values that those calculated by linear analysis. Also, it can be seen that the peak value of each curve does not occur at the same  $Vt/a$ . Moreover, variation of the value of these peak points for moving mass and moving force problem have an increasing trend up to the velocity ratio  $\alpha = 1.25$  and a reverse trend afterward no matter what type of analysis is used. For the load velocity ratio of  $\alpha \geq 0.75$ , the position of the peak point shifts to the right end as  $\alpha$  increases. In addition, it is seen that for higher velocity ratio, i.e.  $\alpha \geq 2.5$ , the vertical dynamic displacement of the plate's central point yields to a small value at the time of leaving the plate which means the plate does not have enough time to respond accordingly against the fast speed of the moving mass/force. Another interesting observation from Fig. 10 is related to the interaction between the plate's central point displacement and load speed for example with the load velocity ratio of  $\alpha = 1$  for the moving mass problem and moving force problem and there is a reverse (upward) displacement for the central point which happens usually when the load leaves the plate.

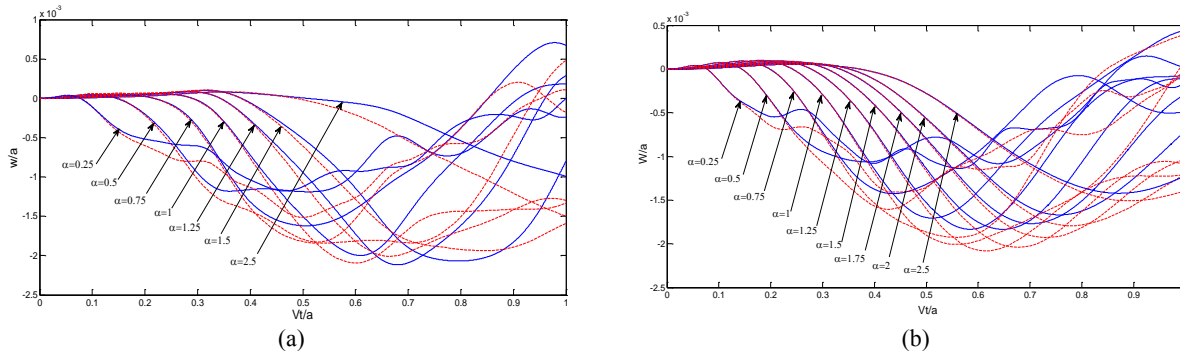


**Fig.10**  
Time histories for normalized central point deflection of a plate subjected to: (a) a moving mass of  $m_e=0.25\mu ab$  (kg), (b) a moving force of  $F=0.25\mu gab$  (N); (—) nonlinear analysis, (----) linear analysis.

## 5 CONCLUSIONS

Three nonlinear coupled PDEs of motion for the in-plane and out of plane displacements of a rectangular simply supported plate subjected to a traveling mass and as well as an equivalent concentrated force solved and the results are as follows:

1. It can be seen that the size of D.M.F. using nonlinear analysis almost higher value than those given by linear analysis, hence the difference between the D.M.F. response of the nonlinear and linear theories increases.
2. It can be observed that the dynamic of central point displacements of a moving mass/force problem using linear and nonlinear solutions are almost the same for the smaller values of  $m_e$  or  $F$ . However, the magnitude of the plate deflection of the nonlinear and the linear solutions differs gradually and the difference grows rapidly as the value of  $m_e$  or  $F$  increases, respectively.
3. It can be seen that maximum dynamic displacement variation ( $w$ ) of central point of plate vs. different value of the mass/force ratios  $\eta$  of the linear solution mathematically follows a linear trend in a moving force problem, whereas this variation does not represent a linear trend in a moving mass problem.
4. It can be observed that by increasing the aspect ratio of the rectangular plate, the maximum value of the dynamic magnification factor decreases and occurs in the lower values of  $\alpha$ .

## APPENDIX A

$$\begin{aligned}
 I_{1,ij} &= \int_0^b \int_0^a \frac{d^2 \phi_{ij}(x,y)}{dx^2} \phi_{ij}(x,y) dx dy & I_{2,yz} &= \int_0^b \int_0^a \frac{d \theta_{yz}(x,y)}{dx} \frac{d^2 \theta_{yz}(x,y)}{dx^2} \phi_{ij}(x,y) dx dy \\
 I_{3,kl} &= \int_0^b \int_0^a \frac{d^2 \psi_{kl}(x,y)}{dx dy} \phi_{ij}(x,y) dx dy & I_{4,yz} &= \int_0^b \int_0^a \frac{d \theta_{yz}(x,y)}{dy} \frac{d^2 \theta_{yz}(x,y)}{dx dy} \phi_{ij}(x,y) dx dy \\
 I_{5,ij} &= \int_0^b \int_0^a \frac{d^2 \phi_{ij}(x,y)}{dy^2} \phi_{ij}(x,y) dx dy & I_{6,yz} &= \int_0^b \int_0^a \frac{d \theta_{yz}(x,y)}{dx} \frac{d^2 \theta_{yz}(x,y)}{dy^2} \phi_{ij}(x,y) dx dy \\
 I_{7,ij} &= \int_0^b \int_0^a \phi_{ij}^2(x,y) dx dy & I_{8,kl} &= \int_0^b \int_0^a \frac{d^2 \psi_{kl}(x,y)}{dy^2} \psi_{kl}(x,y) dx dy \\
 I_{9,yzkl} &= \int_0^b \int_0^a \frac{d \theta_{yz}(x,y)}{dy} \frac{d^2 \theta_{yz}(x,y)}{dy^2} \psi_{kl}(x,y) dx dy & I_{10,ijkl} &= \int_0^b \int_0^a \frac{d^2 \phi_{ij}(x,y)}{dx dy} \psi_{kl}(x,y) dx dy \\
 I_{11,yzkl} &= \int_0^b \int_0^a \frac{d \theta_{yz}(x,y)}{dx} \frac{d^2 \theta_{yz}(x,y)}{dx dy} \psi_{kl}(x,y) dx dy & I_{12,kl} &= \int_0^b \int_0^a \frac{d^2 \psi_{kl}(x,y)}{dx^2} \psi_{kl}(x,y) dx dy \\
 I_{13,yzkl} &= \int_0^b \int_0^a \frac{d \theta_{yz}(x,y)}{dy} \frac{d^2 \theta_{yz}(x,y)}{dx^2} \psi_{kl}(x,y) dx dy & I_{14,yzkl} &= \int_0^b \int_0^a \psi_{kl}^2(x,y) dx dy \\
 I_{15,yz} &= \int_0^b \int_0^a \frac{d^4 \theta_{yz}(x,y)}{dx^4} \theta_{yz}(x,y) dx dy & I_{16,yz} &= \int_0^b \int_0^a \frac{d^4 \theta_{yz}(x,y)}{dx^2 dy^2} \theta_{yz}(x,y) dx dy \\
 I_{17,yz} &= \int_0^b \int_0^a \frac{d^4 \theta_{yz}(x,y)}{dy^4} \theta_{yz}(x,y) dx dy & I_{18,ijvz} &= \int_0^b \int_0^a \frac{d \phi_{ij}(x,y)}{dx} \frac{d^2 \theta_{yz}(x,y)}{dx^2} \theta_{yz}(x,y) dx dy
 \end{aligned}$$

$$\begin{aligned}
 I_{19,vz} &= \int_0^b \int_0^a \left( \frac{d\theta_{vz}(x,y)}{dx} \right)^2 \frac{d^2\theta_{vz}(x,y)}{dx^2} \theta_{vz}(x,y) dx dy & I_{20,klvz} &= \int_0^b \int_0^a \frac{d\psi_{kl}(x,y)}{dy} \frac{d^2\theta_{vz}(x,y)}{dy^2} \theta_{vz}(x,y) dx dy \\
 I_{21,vz} &= \int_0^b \int_0^a \left( \frac{d\theta_{vz}(x,y)}{dy} \right)^2 \frac{d^2\theta_{vz}(x,y)}{dy^2} \theta_{vz}(x,y) dx dy & I_{22,klvz} &= \int_0^b \int_0^a \frac{d\psi_{kl}(x,y)}{dy} \frac{d^2\theta_{vz}(x,y)}{dx^2} \theta_{vz}(x,y) dx dy \\
 I_{23,vz} &= \int_0^b \int_0^a \left( \frac{d\theta_{vz}(x,y)}{dy} \right)^2 \frac{d^2\theta_{vz}(x,y)}{dx^2} \theta_{vz}(x,y) dx dy & I_{24,ijvz} &= \int_0^b \int_0^a \frac{d\phi_{ij}(x,y)}{dx} \frac{d^2\theta_{vz}(x,y)}{dy^2} \theta_{vz}(x,y) dx dy \\
 I_{25,vz} &= \int_0^b \int_0^a \left( \frac{d\theta_{vz}(x,y)}{dx} \right)^2 \frac{d^2\theta_{vz}(x,y)}{dy^2} \theta_{vz}(x,y) dx dy & I_{26,ijvz} &= \int_0^b \int_0^a \frac{d\phi_{ij}(x,y)}{dy} \frac{d^2\theta_{vz}(x,y)}{dx dy} \theta_{vz}(x,y) dx dy \\
 I_{27,klvz} &= \int_0^b \int_0^a \frac{d\psi_{kl}(x,y)}{dx} \frac{d^2\theta_{vz}(x,y)}{dx dy} \theta_{vz}(x,y) dx dy & I_{28,vz} &= \int_0^b \int_0^a \frac{d\theta_{vz}(x,y)}{dx} \frac{d\theta_{vz}(x,y)}{dy} \frac{d^2\theta_{vz}(x,y)}{dx dy} \theta_{vz}(x,y) dx dy \\
 I_{29,ijvz} &= \int_0^b \int_0^a \frac{d\theta_{vz}(x,y)}{dx} \phi_{ij}(x,y) \theta_{vz}(x,y) dx dy & I_{30,klvz} &= \int_0^b \int_0^a \frac{d\theta_{vz}(x,y)}{dy} \psi_{kl}(x,y) \theta_{vz}(x,y) dx dy \\
 I_{31,vz} &= \int_0^b \int_0^a \theta_{vz}^2(x,y) dx dy & I_{32,vz} &= \theta_{vz}(x = x_0(t), y = b/2) \\
 I_{33,vz} &= \frac{d^2\theta_{vz}(x = x_0(t), y = b/2)}{dx^2} \theta_{vz}(x = x_0(t), y = b/2) & I_{34,vz} &= \theta_{vz}^2(x = x_0(t), y = b/2) \\
 I_{35,vz} &= \frac{d\theta_{vz}(x = x_0(t), y = b/2)}{dx} \theta_{vz}(x = x_0(t), y = b/2)
 \end{aligned}$$

REFERENCES

- [1] Amabili M., 2004, Nonlinear vibrations of rectangular plates with different boundary conditions: theory and experiments, *Computers and Structures* **82**: 2587-2605.
- [2] Eftekhari S.A., Jafari A.A., 2012, Vibration of an initially stressed rectangular plate due to an accelerated traveling mass, *Scientia Iranica* **19**(5):1195-1213.
- [3] Fryba L., 1999, *Vibration of Solids and Structures under Moving Loads*, Thomas Telford Publishing, London.
- [4] Gbadeyan J.A., Oni S.T., 1995, Dynamic behaviour of beams and rectangular plates under moving loads, *Journal of Sound and Vibration* **182**(5): 677-695.
- [5] Ghafoori E., Kargarnovin M.H., Ghahremani A.R., 2010, Dynamic responses of rectangular plate under motion of an oscillator using a semi-analytical method, *Journal of Vibration and Control* **17**(9): 1310-1324.
- [6] Kiani K.A., Nikkhoo A., Mehri B., 2009, Prediction capabilities of classical and shear deformable beam models excited by a moving mass, *Journal of Sound and Vibration* **320**: 632-648.
- [7] Leissa A.W., 1969, *Vibration of Plates*, US Government Printing Office, Washington.
- [8] Mamandi A., Kargarnovin M.H., Younesian D., 2010, Nonlinear dynamics of an inclined beam subjected to a moving load, *Nonlinear Dynamics* **60**(3): 277-293.
- [9] Mamandi A., Kargarnovin M.H., 2014, An investigation on dynamic analysis of a Timoshenko beam with geometrical nonlinearity included resting on a nonlinear viscoelastic foundation and traveled by a moving mass, *Shock and Vibration* **24**2090:1-10.
- [10] Mamandi A., Kargarnovin M.H., Farsi S., 2014, Nonlinear vibration solution of an inclined Timoshenko beam under the action of a moving force with constant/non-constant velocity, *Journal of Mathematical Sciences* **201**(3): 361-383.
- [11] Mamandi A., Kargarnovin M.H., 2011, Nonlinear dynamic analysis of an inclined Timoshenko beam subjected to a moving mass/force with beam's weight included, *Shock and Vibration* **18**(6): 875-891.
- [12] Mamandi A., Kargarnovin M.H., 2011, Dynamic analysis of an inclined Timoshenko beam travelled by successive moving masses/forces with inclusion of geometric nonlinearities, *Acta Mechanica* **218**(1):9-29.

- [13] Mamandi A., Kargarnovin M.H., Farsi S., 2010, An investigation on effects of a traveling mass with variable velocity on nonlinear dynamic response of an inclined Timoshenko beam with different boundary conditions, *International Journal of Mechanical Sciences* **52**(12):1694-1708.
- [14] Mamandi A., Kargarnovin M.H., 2013, Nonlinear dynamic analysis of an axially loaded rotating Timoshenko beam with extensional condition included subjected to general type of force moving along the beam length, *Journal of Vibration and Control* **19**(16): 2448-2458.
- [15] Meirovitch L., 1997, *Principles and Techniques of Vibrations*, Prentice-Hall Inc., New Jersey.
- [16] Nayfeh A.H., Mook D.T., 1995, *Nonlinear Oscillations*, Wiley-Interscience, New York.
- [17] Nikkhoo A., Rofooei F.R., 2012, Parametric study of the dynamic response of thin rectangular plates traversed by a moving mass, *Acta Mechanica* **223**: 15-27.
- [18] Shadnam M.R., Mofid M., Akin J.E., 2001, On the dynamic response of rectangular plate with moving mass, *Thin-walled Structures* **39**: 797-806.
- [19] Timoshenko S.P., 1959, *Theory of Plates and Shells*, Mc Graw-Hill, New York.
- [20] Vaeseghi Amiri J., Nikkhoo A., Davoodi M.R., Ebrahimzadeh Hassanabadi M., 2013, Vibration analysis of a Mindlin elastic plate under a moving mass excitation by eigenfunction expansion method, *Thin-Walled Structures* **62**: 53-64.
- [21] Wu J.J., 2007, Vibration analyses of an inclined flat plate subjected to moving loads, *Journal of Sound and Vibration* **299**: 373-387.
- [22] Yanmeni Wayou A.N., Tchoukuegno R., Wofo P., 2004, Non-linear dynamics of an elastic beam under moving loads, *Journal of Sound and Vibration* **273**: 1101-1108.
- [23] Mamandi A., Kargarnovin M.H., Mohsenzadeh R., 2015, Nonlinear dynamic analysis of a rectangular plate subjected to accelerated/decelerated moving load, *Journal of Theoretical and Applied Mechanics* **53**(1):151-166.